This paper was presented as part of the main technical program at IEEE INFOCOM 2011

Downlink Power Control for Variable Bit Rate Videos over Multicell Wireless Networks

Yingsong Huang and Shiwen Mao
Department of Electrical and Computer Engineering, Auburn University, Auburn, AL

***Abstract*—We investigate the problem of downlink power control for streaming multiple variable bit rate (VBR) videos in a multicell wireless network, where downlink capacities are limited by inter-cell interference. We adopt a deterministic model for VBR traffic that considers video frame sizes and playout buffers at the mobile users. The problem is to find the optimal transmit powers for the base stations, such that VBR video data can be delivered to mobile users without causing playout buffer underflow or overflow. We formulate a nonlinear nonconvex optimization problem and prove the condition for the existence of feasible solutions. We then develop a centralized branch-and-bound algorithm incorporating the Reformulation-Linearization Technique, which can produce (1-ϵ)-optimal solutions. We also propose a low-complexity distributed algorithm with fast convergence. Through simulations with VBR video traces under fading channels, we find the distributed algorithm can achieve a performance very close to that of the centralized algorithm.**

I. Introduction

With the dramatic advances in wireless networking technology and wireless communication devices, there is an exponentially increasing demand for wireless video service. According to a recent study by Cisco [1], mobile data traffic will double every year through 2014, increasing 39 times between 2009 and 2014 globally. In addition, video will account for 66% of the mobile data traffic by 2014. This trend is driven by the compelling need for ubiquitous access to video content over wireless access networks, and will significantly stress the capacity of existing wireless networks and strongly influence the design of future wireless networks.

Significant effort is needed in wireless video research to meet this tremendous demand. While it is important to develop new wireless architectures and technologies for higher spectral efficiency, it is equally important to investigate how to support video in existing wireless networks, since the infrastructure will still last for a considerable period of time. In this paper, we consider video streaming over a multicell wireless network, a wireless network architecture widely deployed all over the world. We consider the typical case of downlink video transmissions. For the multicell system, generally intra-cell interference can be effectively controlled with precise synchronization or the use of guard times. The capacities of the downlinks are mainly limited by the inter-cell interference due to simultaneous base station (BS) transmissions using the same channel. Therefore, effective downlink power control is necessary to support concurrent videos.

We consider the problem of streaming concurrent variable-bit-rate (VBR) videos in the multicell wireless network. This is motivated by the superior perceived quality of VBR videos over constant-bit-rate (CBR) videos. VBR video has stable visual quality for the frames, but at the cost of large variations in the bit rate, while CBR video maintains a stable bit rate, but the frames have large variations in visual quality. Due to this reason, many stored videos are VBR. We aim to investigate how to provide ubiquitous access to such stored VBR videos through existing cellular networks.

It is a challenging problem to support VBR video traffic, which is found to exhibit both strong long-range and short-range-dependence [2], [3]. It is nontrivial to develop parsimonious traffic models that can accurately capture the auto-correlation structure. The large frame size variations may cause frequent playout buffer underflow or overflow. To address this issue, we adopt a deterministic traffic model for stored VBR video, which considers frame size, frame rate, and playout buffers [4]–[7]. Unlike prior work that is focused on a single video session over a given CBR or VBR channel, we exploit power control, a unique capability in wireless networks, to adjust the downlink capacities based on prior knowledge of frame sizes and playout schedules. Usually large frames are rarely transmitted simultaneously. Thus jointly optimizing the BS transmit powers is, in some sense, analogous to statistical multiplexing VBR videos in the multicell network.

We presented a problem formulation that considers downlink power control, inter-cell interference, VBR video characteristics, and playout buffer requirements. The objective is to achieve high playout buffer utilization, under playout buffer underflow and overflow constraints and peak power constraint. This is a nonlinear nonconvex problem to which traditional convex optimization techniques [8] and low- or high-SINR approximations [8], [9] do not directly apply.

In this paper, we first derive the condition of the existence of feasible power assignments, which can achieve downlink capacities to guarantee no buffer underflow and overflow. We then develop a centralized algorithm that can produce solutions with bounded optimality gap. Specifically, we use the Linearization-Reformulation Technique (RLT) to obtain a linear programming (LP) relaxation of the original problem. Solving this LP relaxation yields an upper bound to the original problem. Interestingly, since the constraints are preserved in the relaxation procedure, the upper-bounding solution is also feasible to the original problem; the corresponding objective value with this solution provides a lower bound to the global optimum. The LP relaxation is then incorporated into the branch-and-bound framework to obtain a centralized

978-1-4244-9921-2/11/$26.00 ©2011 IEEE

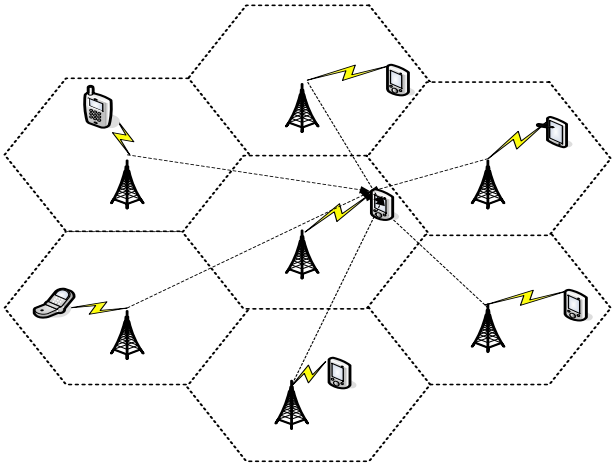

Fig. 1. A multicell wireless network with concurrent VBR video sessions. The inter-cell interference experienced by the central cell user is illustrated.

algorithm, which can produce a solution within the (1-ϵ) range of the global optimal.

To simplify computation and control, we also develop a distributed algorithm based on distributed constrained power control (DCPC) [10], where each BS iteratively updates transmit power based on feedback of measured SINR at the target receiver. It is shown that with DCPC, the power vector converges to a unique power vector that can achieve the goal of maximizing playout buffer utilization and avoiding playout buffer underflow and overflow. We evaluate the proposed algorithms with simulations using VBR video traces [11] and fading channels. The distributed algorithm is shown to achieve a performance very close to that of the centralized algorithm. Both algorithms are demonstrated to be highly effective for streaming VBR videos over multicell wireless networks.

In the reminder of this paper, we present the problem formulation in Section II. We describe a centralized algorithm in Section III and a distributed algorithm in Section IV. Simulation results are presented in Section V and related work is discussed in Section VI. Section VII concludes this paper.

II. Problem Statement

A. Network and Video System Model

We consider the downlinks of an M-cell wireless network as shown in Fig. 1. In each cell, a BS streams video to mobile users in the cell, each allocated with a downlink channel. A channel is a spectral resource slot, the nature of which depends on the specific multiple access technique adopted for the multicell network. Without loss of generality, we assume that the downlink channels within a cell are orthogonal (e.g., due to perfect synchronization of spreading codes or use of guard times). The main interference at a user stems from the concurrent downlink transmissions in neighboring cells that use the same channel. There is a need for the BS's to adopt power control to mitigate such inter-cell interference.

We consider the problem of streaming multiple VBR videos in the multicell network. We assume the wired segment of a video session path is reliable with sufficient bandwidth, while the last-hop wireless link is the bottleneck [12]. Thus the corresponding video data is always available at the BS before the scheduled transmission time.

It is non-trivial to accurately model VBR video traffic, which exhibits both strong asymptotic self-similarity and short-range correlation [2]. A stochastic model capturing the auto-correlation structure often requires a large number of parameters, and is thus hard to be incorporated for scheduling real-time video data. To this end, we adopt a *deterministic model* that considers frame sizes, playout buffers, and schedule [5]. Let $D_i(t)$ denote the *cumulative consumption curve* of the i-th user, representing the cumulative amount of bits consumed by the decoder at time t. The cumulative consumption curve is determined by video characteristics such as frame sizes and rates, and playout schedule. Assume user i has a playout buffer of size b_i bits and its video has L_i frames. We can derive a *cumulative overflow curve* for user i as

$$B_i(t) = \min\{D_i(t-1) + b_i, D_i(L_i)\},\ 0 \le t \le L_i. \quad (1)$$

$B_i(t)$ is the maximum number of cumulative received bits at time t without overflowing user i's playout buffer. Finally we define *cumulative transmission curve* $X_i(t)$ as the cumulative amount of bits transmitted to user i at time t. To simplify notation, we assume the video sessions have identical frame rate and the frame intervals are synchronized. Thus a time slot t is equal to the t-th frame interval, denoted as τ, for $0 \le t \le \max_i\{L_i\}$.[1]

Since $D_i(t)$, $B_i(t)$ and $X_i(t)$ are cumulative curves, they are all nondecreasing functions of time. The three curves are illustrated in Fig. 2. A feasible transmission schedule will produce a cumulative transmission curve $X_i(t)$ that lies within $D_i(t)$ and $B_i(t)$, i.e., causing neither underflow nor overflow at the playout buffer. In practice, $D_i(t)$'s are known for stored videos and are delivered to the BS's (or a centralized video scheduler) during the session setup phase, and $B_i(t)$'s are then derived as in (1).

B. Problem Formation

For the multicell wireless video network, consider a specific channel and let $\mathcal{U} = \{un_1, un_2, \cdots, un_M\}$ denote the set of users sharing the channel, where un_m is the user in cell m.[2] Let the BS *transmit power vector* be $\vec{P}(t) = [P_1(t), P_2(t), \cdots, P_M(t)]^T$ in time slot t. The capacity of the downlink from BS m to user un_m, denoted as $C_m(t)$, depends on the SINR at un_m, which can be written as

$$\gamma_m(\vec{P}(t)) = \frac{G_m^m P_m(t)}{\sum_{k \ne m} G_k^m P_k(t) + \eta_m}, \quad (2)$$

[1] For example, if the frame rates are different, we can use a time slot duration that is equal to the greatest common divisor of all the frame intervals (if not too small). If the frame intervals are not synchronized, a time slot can be a fraction of a frame interval within which the $D_i(t)$'s of all the videos remain constant. In fact, the time slot duration could be arbitrary as in [13] (i.e., equal to multiple frame intervals). Since the cumulative overflow and consumption curves are known, we can still determine the upper and lower bounds for the transmission rate in each time slot. The problem formulation and proposed solution procedures to be discussed in the following sections apply to these cases.

[2] 0-1 index variables can be used to model the case where no user uses the channel in some cells, but are omitted for brevity.

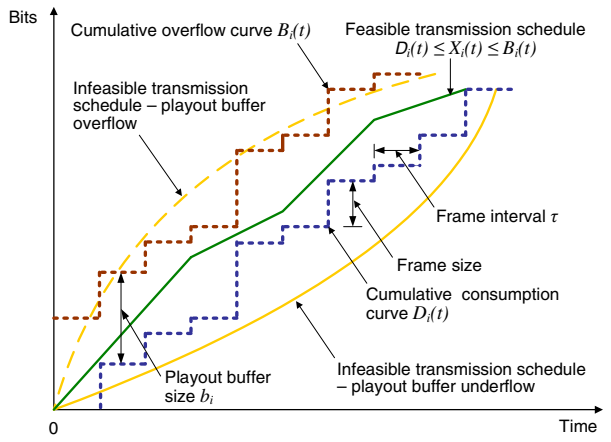

Fig. 2. Feasible and infeasible transmission schedules for video session i.

where G_k^m is the path gain from BS k to user un_m and η_m is the noise power at un_m. We assume slow-fading channels such that the path gains do not change within each time slot [13], but vary over different time slots following a certain distribution. The downlink capacity $C_m(t)$ also depends on the channel bandwidth B_w and the transceiver design, such as modulation and channel coding. Without loss of generality, we use the upper bound as predicted by Shannon theorem:

$$C_m(\vec{P}(t)) = B_w \log\left(1 + \gamma_m(\vec{P}(t))\right). \quad (3)$$

The impact of fading channels is incorporated in the SINR in (3). For practical systems, the achievable capacity may be a fraction of $C_m(\vec{P}(t))$, but this part is omitted for brevity.

Once the link capacity is determined, $C_m(t)\tau$ video bits will be delivered to user un_m in that time slot. The cumulative transmission curve $X_m(t)$ can be written as

$$X_m(0) = 0; \;\; X_m(t) = X_m(t-1) + C_m(t)\tau. \quad (4)$$

Assume peak power constraint $0 \le P_m \le \bar{P}$, for all m. The problem is to determine the transmit power vector $\vec{P}(t)$, for $0 < t \le \max_i\{L_i\}$, such that the resulting cumulative transmission curves satisfy

$$D_m(t) \le X_m(t) \le B_m(t), \;\; \text{for all } m, t, \quad (5)$$

i.e., without causing playout buffer underflow or overflow. Since the video frames have variable sizes and the video sessions have random phases, large frames from different sessions are less likely to occur in the same time slot. Jointly considering power control for the downlinks is, in some sense, analogous to statistical multiplexing of VBR video flows.

From (3)∼(5), the feasible SINR range at user un_m is

$$e^{\frac{\max\{0, D_m(t) - X_m(t-1)\}}{B_w \tau}} - 1 \le \gamma_m \le e^{\frac{B_m(t) - X_m(t-1)}{B_w \tau}} - 1. \quad (6)$$

In (6), the lower bound is the SINR that just empties the buffer without causing underflow. The upper bound is the SINR that just fills up the buffer without causing overflow.

Generally, the feasible transmit power vector $\vec{P}(t)$ is not unique for a given set of VBR video sessions. Among the set of feasible solutions, a schedule that transmits more data is more desirable since it provides a larger search space for optimizing transmit power vectors for future time slots. Omitting the constant B_w, we formulate the optimal power control problem for VBR videos, termed Problem OPT-VBR, as

$$\textbf{maximize} \quad \sum_{m \in \mathcal{U}} \log(1 + \gamma_m(t)) \quad (7)$$

$$\textbf{subject to:} \quad \gamma_m(t) = \frac{G_m^m P_m(t)}{\sum_{k \ne m} G_k^m P_k(t) + \eta_m}, \; \forall\, m \quad (8)$$

$$\gamma_m^{min}(t) \le \gamma_m(t) \le \gamma_m^{max}(t), \; \forall\, m \quad (9)$$

$$0 \le P_m \le \bar{P}, \; \forall\, m, \quad (10)$$

where $\gamma_m^{max}(t)$ is the upper bound in (6) and $\gamma_m^{min}(t)$ is the larger one between the lower bound in (6) and γ_m^{th}, a minimum SINR requirement imposed by the transceiver design.

In Problem OPT-VBR, the total amount of video data delivered in time slot t is maximized, under playout buffer underflow and overflow constraints and peak transmit power constraints. This is a nonlinear nonconvex problem, to which traditional convex optimization techniques do not directly apply. Furthermore, to achieve the objective of avoiding playout buffer underflow and overflow, the SINRs may assume values ranging from very low to very high. Thus the existing high SINR approximation [8] and low SINR approximation [9] techniques cannot be used. In the following, we first prove the existence of feasible solutions. We then derive effective centralized and distributed algorithms to solve Problem OPT-VBR in Sections III and IV.

C. Existence of Feasible Solutions

Due to the wide range of VBR video frame sizes, the corresponding SINR requirements also assume a wide range of values. Under conditions where many video sessions coincidently transmit their large frames in the same time slot, Problem OPT-VBR may not have a feasible power assignment to deliver all the frames. In this section, we derive the conditions for the existence of feasible power assignments. We assume a centralized scheduler in the multicell network, which has prior knowledge of all the path gains and the cumulative consumption and overflow curves.

We define the *minimum required rate* for user un_m in time slot t, denoted as $C_m^{min}(t)$, as the bit rate such that the playout buffer is just emptied, but without underflow, at the end of time slot t. We have the following result for $C_m^{min}(t)$.

Lemma 1: The largest value for the minimum required rate $C_m^{min}(t)$ is $\bar{C}_m^{min}(t) = [D_m(t) - D_m(t-1)]/\tau$.

Proof: According to the definition of $X_m(t)$ in (4), we have $C_m(t) = [X_m(t) - X_m(t-1)]/\tau$. From the definition of $C_m^{min}(t)$, the playout buffer is emptied at the end of time slot t, i.e., $X_m(t) = D_m(t)$. Therefore, we can derive the minimum required rate as

$$C_m^{min}(t) = \max\{0, D_m(t) - X_m(t-1)\}/\tau. \quad (11)$$

From the feasibility condition (5), we have $X_m(t-1) \ge D_m(t-1)$. Substituting it into (11), we have

$$C_m^{min}(t) \le [D_m(t) - D_m(t-1)]/\tau \equiv \bar{C}_m^{min}(t). \quad (12)$$

Rate $\bar{C}_m^{min}(t)$ occurs when the playout buffer is empty at both the beginning and end of time slot t, but without buffer overflow during the entire time slot. ■

We have the following condition for the existence of a feasible power assignment for Problem OPT-VBR.

Theorem 1: There exits a feasible power assignment for Problem OPT-VBR for time slot t, if there exits a feasible power assignment that can achieve the rate vector $\left[\bar{C}_1^{min}(t), \bar{C}_2^{min}(t), \cdots, \bar{C}_M^{min}(t)\right]$.

Proof: Recall that γ_m^{min} is the SINR corresponding to the minimum required rate $C_m^{min}(t)$. Let $\bar{\gamma}_m^{min}(t)$ be the SINR corresponding to $\bar{C}_m^{min}(t)$. Since (3) is a monotonically increasing function, we have $0 \leq \gamma_m^{min}(t) \leq \bar{\gamma}_m^{min}(t)$.

We now consider the power assignment that achieves rates $\bar{C}_m^{min}(t)$, or, the corresponding SINRs $\bar{\gamma}_m^{min}(t)$. From (8) and (9), the minimum SINR constraint is:

$$\gamma_m(t) = \frac{G_m^m P_m(t)}{\sum_{k \neq m} G_k^m P_k(t) + \eta_m} \geq \bar{\gamma}_m^{min}(t), \ \forall \ m. \quad (13)$$

Eqn. (13) is a system of linear equations of the power vector $\vec{P}(t)$, which can be written in the matrix form as:

$$\left(\mathbf{I} - \bar{\mathbf{\Gamma}}^{min}\mathbf{A}\right)\vec{P}(t) \succeq \bar{\mathbf{\Gamma}}^{min}\vec{\nu}, \quad (14)$$

where $\mathbf{I}$ is the identity matrix, $\mathbf{A}$ is an $M \times M$ matrix with

$$A_{mk} = \begin{cases} 0, & m = k \\ G_k^m / G_m^m, & m \neq k, \end{cases} \quad (15)$$

$\bar{\mathbf{\Gamma}}^{min} = \text{diag}\{\bar{\gamma}_1^{min}(t), \bar{\gamma}_2^{min}(t), \cdots, \bar{\gamma}_M^{min}(t)\}$ is a diagonal matrix, and $\vec{\nu} = [\eta_1/G_1^1, \eta_2/G_2^2, \cdots, \eta_M/G_M^M]^T$.

Define $\mathbf{\Gamma}^{min} = \text{diag}\{\gamma_1^{min}(t), \gamma_2^{min}(t), \cdots, \gamma_M^{min}(t)\}$ and $\mathbf{\Delta} = \bar{\mathbf{\Gamma}}^{min} - \mathbf{\Gamma}^{min} \succeq \mathbf{0}$. Assume $\vec{P}$ is a power assignment that achieves $\bar{\gamma}_m^{min}(t)$ for all m, which satisfies (14). Substituting $\bar{\mathbf{\Gamma}}^{min} = \mathbf{\Delta} + \mathbf{\Gamma}^{min}$ into (14), we have

$$\left(\mathbf{I} - \mathbf{\Gamma}^{min}\mathbf{A}\right)\vec{P} \succeq \mathbf{\Gamma}^{min}\vec{\nu} + \mathbf{\Delta}\left(\vec{\nu} + \mathbf{A}\vec{P}\right).$$

Since $\mathbf{\Delta}$, $\vec{\nu}$, $\mathbf{A}$ and $\vec{P}$ all have non-negative elements, we have $\mathbf{\Delta}\left(\vec{\nu} + \mathbf{A}\vec{P}\right) \succeq \mathbf{0}$, and therefore,

$$\left(\mathbf{I} - \mathbf{\Gamma}^{min}\mathbf{A}\right)\vec{P} \succeq \mathbf{\Gamma}^{min}\vec{\nu}. \quad (16)$$

That is, $\vec{P}$ can also achieve $\gamma_m^{min}(t)$ for all m and it satisfies the minimum SINR constraint in (9).

Once the minimum SINR constraint in (9) (i.e., no buffer underflow) is satisfied, the maximum SINR constraint in (9) (i.e., no buffer overflow) can be satisfied since BS m can stop transmission when the playout buffer at user un_m is full. ■

Theorem 1 allows us to evaluate, for a given set of videos, if there is a feasible power assignment for each time slot. There is no need to consider the transmission schedules and playout buffer occupancies in previous time slots. At the beginning of time slot t, we obtain $\bar{\gamma}_m^{min}(t)$ from the cumulative consumption curve $D(t)$ and channel gains. If the linear system (14) is solvable and the resulting $\vec{P}$ satisfies constraint (10), then there is a feasible power assignment for Problem OPT-VBR for this time slot. The following fact from [14] can be used for the feasibility test.

Fact 1: The following statements are equivalent: (i) there exits a feasible power assignment satisfying (14); (ii) the maximum modulus eigenvalue of $\left(\bar{\mathbf{\Gamma}}^{min}\mathbf{A}\right)$ is less than 1; (iii) the reciprocal matrix $(\mathbf{I} - \bar{\mathbf{\Gamma}}^{min}\mathbf{A})^{-1} = \sum_{k=0}^{\infty}\left(\bar{\mathbf{\Gamma}}^{min}\mathbf{A}\right)^k$ exists and is positive component-wise.

III. Centralized Algorithm

As discussed, Problem OPT-VBR is a nonlinear nonconvex problem, to which traditional convex optimization techniques do not directly apply. In this section, we present a centralized algorithm to provide solutions with bounded optimality gap. We first use RLT to obtain a linear programming (LP) relaxation of Problem OPT-VBR [15]. We then incorporate the linear relaxation into a branch-and-bound framework, which can produce (1-ϵ)-optimal solutions.

A. Reformulation and Linearization

We first apply *polyhedral outer approximation* for the logarithm functions in Problem OPT-VBR to obtain a Polynomial Programming Problem OPT-VBR(p) [16]. We then use *RLT bound-factor product constraints* to relax the quadratic terms to obtain an LP relaxation OPT-VBR(l). The time slot index (t) is dropped in the following to simplify notation.

We first process the logarithm functions in the objective function. Letting $u_m = \log(1 + \gamma_m)$, we obtain a linear objective function $\sum_{m \in \mathcal{U}} u_m$ and new constraints $u_m = \log(1 + \gamma_m)$. We deal with the new constraints using polyhedral outer approximation. Since $\gamma_m^{min} \leq \gamma_m \leq \gamma_m^{max}$, we choose H points, denoted as $\{\gamma_m^h\}$, within this range as

$$\gamma_m^h = (1 + \gamma_m^{min})\left(\frac{1 + \gamma_m^{max}}{1 + \gamma_m^{min}}\right)^{\frac{h}{H-1}} - 1, h = 0, \cdots, H-1, \quad (17)$$

where $\gamma_m^0 = \gamma_m^{min}$ and $\gamma_m^{H-1} = \gamma_m^{max}$. We can obtain a *convex envelop* for the logarithm function in $[\gamma_m^{min}, \gamma_m^{max}]$, which consists of H tangent lines at the H points given in (17) and the line segment connecting the two end points. We relax the logarithm constraint by using its convex envelop, represented by the following new linear constraints:

$$\begin{cases} u_m \geq \frac{\log(1+\gamma_m^{min})}{\gamma_m^{max} - \gamma_m^{min}}(\gamma_m^{max} - \gamma_m) + \frac{\log(1+\gamma_m^{max})}{\gamma_m^{max} - \gamma_m^{min}}(\gamma_m - \gamma_m^{min}) \\ u_m \leq \log(1 + \gamma_m^h) + \frac{\gamma_m - \gamma_m^h}{1 + \gamma_m^h}, \ h = 0, 1, \cdots, H-1. \end{cases} \quad (18)$$

The first line is for the segment connecting the two end points, and the second line is for the tangent lines at the H points. A four-point approximation is illustrated in Fig. 3.

With the polyhedral outer approximation, we obtain a polynomial programming problem OPT-VBR(p), as given in (19) $\sim$ (26). We can rewrite the last constraint (26) as

$$\sum_{k \neq m} G_k^m \gamma_m P_k - G_m^m P_m + \eta_m \gamma_m = 0, \quad (27)$$

which contains quadratic terms in the form of $\gamma_m P_k$. We next introduce RLT bound-factor product constraints to remove such terms and to obtain an LP relaxation.

Define substitution variables $v_{mk} = \gamma_m P_k$, for all m, k. Since γ_m and P_k are bounded by their respective lower and

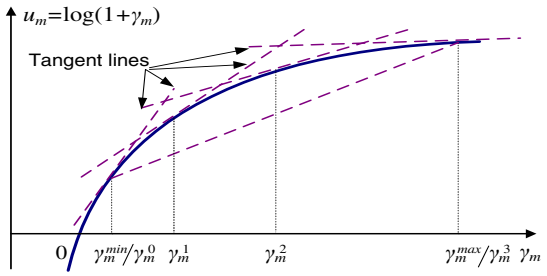

Fig. 3. Four-point polyhedral outer approximation for $u_m = \log(1+\gamma_m)$, $1 < \gamma_m^{min} \le \gamma_m \le \gamma_m^{max}$.

maximize $\sum_{m\in\mathcal{U}} u_m$ (19)

subject to:

$$G_m^m P_m - \left(\sum_{k\neq m} G_k^m P_k + \eta_m\right)\gamma_m^{min} \ge 0,\ \forall\, m \quad (20)$$

$$G_m^m P_m - \left(\sum_{k\neq m} G_k^m P_k + \eta_m\right)\gamma_m^{max} \le 0,\ \forall\, m \quad (21)$$

$$0 \le P_m \le \bar{P},\ \forall\, m \quad (22)$$

$$u_m \ge \frac{\log(1+\gamma_m^{min})}{\gamma_m^{max}-\gamma_m^{min}}(\gamma_m^{max}-\gamma_m) + \frac{\log(1+\gamma_m^{max})}{\gamma_m^{max}-\gamma_m^{min}}(\gamma_m-\gamma_m^{min}),\ \forall\, m \quad (23)$$

$$u_m \le \log(1+\gamma_m^h) + \frac{\gamma_m-\gamma_m^h}{1+\gamma_m^h},\ \forall\, m,h \quad (24)$$

$$\gamma_m^h = (1+\gamma_m^{min})\left(\frac{1+\gamma_m^{max}}{1+\gamma_m^{min}}\right)^{\frac{h}{H-1}} - 1, \forall\, m,h \quad (25)$$

$$\gamma_m = \frac{G_m^m P_m}{\sum_{k\neq m} G_k^m P_k + \eta_m},\ \forall\, m. \quad (26)$$

upper bounds as $\gamma_m^{min} \le \gamma_m \le \gamma_m^{max}$ and $0 \le P_k \le \bar{P}$, we obtain the following RLT bound-factor product constraints

$$\begin{cases} (\gamma_m-\gamma_m^{min})\cdot(P_k-0) \ge 0 \\ (\gamma_m^{max}-\gamma_m)\cdot(P_k-0) \ge 0 \\ (\gamma_m-\gamma_m^{min})\cdot(\bar{P}-P_k) \ge 0 \\ (\gamma_m^{max}-\gamma_m)\cdot(\bar{P}-P_k) \ge 0. \end{cases} \quad (28)$$

Substituting $\gamma_m P_k = v_{mk}$, we obtain the following four linear constraints for v_{mk}:

$$\begin{cases} v_{mk} - \gamma_m^{min} P_k \ge 0 \\ \gamma_m^{max} P_k - v_{mk} \ge 0 \\ \gamma_m \bar{P} - v_{mk} - \gamma_m^{min}\bar{P} + \gamma_m^{min} P_k \ge 0 \\ \gamma_m^{max}\bar{P} - \gamma_m^{max} P_k - \gamma_m \bar{P} + v_{mk} \ge 0. \end{cases} \quad (29)$$

The quadratic terms $P_k\gamma_m$ are thus replaced with v_{mk} with the above linear RLT bound-factor constraints, and an LP relaxation OPT-VBR(l) is obtained as given in (30) $\sim$ (41).

The LP relaxation OPT-VBR(l) can be effectively solved with an LP solver in polynomial time. The optimal solution to the LP relaxation consists of $\{\vec{P}^*, \vec{u}^*, \vec{\gamma}^*, \vec{v}^*\}$. It is worth noting that during the reformulation and linearization procedure, we mainly relax the logarithm function in the objective function of OPT-VBR. The original constraints of OPT-VBR are preserved in OPT-VBR(l). Therefore, we have the following theorem regarding the feasibility of the solution, which greatly simplifies the *local search* procedure of the branch-and-bound algorithm to be presented in Section III-B.

maximize $\sum_{m\in\mathcal{U}} u_m$ (30)

subject to:

$$G_m^m P_m - \left(\sum_{k\neq m} G_k^m P_k + \eta_m\right)\gamma_m^{min} \ge 0,\ \forall\, m \quad (31)$$

$$G_m^m P_m - \left(\sum_{k\neq m} G_k^m P_k + \eta_m\right)\gamma_m^{max} \le 0,\ \forall\, m \quad (32)$$

$$0 \le P_m \le \bar{P},\ \forall\, m \quad (33)$$

$$u_m \ge \frac{\log(1+\gamma_m^{min})}{\gamma_m^{max}-\gamma_m^{min}}(\gamma_m^{max}-\gamma_m) + \frac{\log(1+\gamma_m^{max})}{\gamma_m^{max}-\gamma_m^{min}}(\gamma_m-\gamma_m^{min}),\ \forall\, m \quad (34)$$

$$u_m \le \log(1+\gamma_m^h) + \frac{\gamma_m-\gamma_m^h}{1+\gamma_m^h},\ \forall\, m,h \quad (35)$$

$$\gamma_m^h = (1+\gamma_m^{min})\left(\frac{1+\gamma_m^{max}}{1+\gamma_m^{min}}\right)^{\frac{h}{H-1}} - 1, \forall\, m,h \quad (36)$$

$$v_{mk} - \gamma_m^{min} P_k \ge 0,\ \forall\, m, k\neq m \quad (37)$$

$$(\gamma_m-\gamma_m^{min})\bar{P} - v_{mk} + \gamma_m^{min} P_k \ge 0,\ \forall\, m, k\neq m \quad (38)$$

$$\gamma_m^{max} P_k - v_{mk} \ge 0,\ \forall\, m, k\neq m \quad (39)$$

$$(\gamma_m^{max}-\gamma_m)\bar{P} - \gamma_m^{max} P_k + v_{mk} \ge 0,\ \forall\, m, k\neq m \quad (40)$$

$$\sum_{k\neq m} v_{mk} G_k^m - G_m^m P_m + \eta_m\gamma_m = 0,\ \forall\, m. \quad (41)$$

Theorem 2: The optimal transmit power vector $\vec{P}^*$ to the LP relaxation OPT-VBR(l) is a feasible solution to the original problem OPT-VBR.

B. Branch-and-Bound Algorithm

According to Theorem 2, we can substitute the optimal power assignment $\vec{P}^*$ for the LP relaxation into Problem OPT-VBR to obtain a lower bound, while the LP solution itself provides an upper bound. We next incorporate the LP relaxation into a branch-and-bound framework to obtain an algorithm that can produce (1-ϵ)-optimal solutions.

Branch-and-bound is an iterative method for solving optimization problems, especially for discrete and combinatorial problems. A branch-and-bound procedure has two key components. The first one, called *branching*, is to partition a problem into subproblems. The procedure is repeated recursively to each of the subproblems and all produced subproblems naturally form a tree structure, i.e., the *branch-and-bound tree*. Its nodes are the constructed subproblems. The leaves of the tree is also call the *Problem List*. The other component is *bounding*, which is a fast way of finding upper and lower bounds for the optimal solution for each subproblem. For a maximization problem, an infeasible upper bound (UB) can be found by solving a relaxed problem. A *local search* algorithm is then used to explore the neighborhood, to find a feasible lower-bounding solution (LB). As discussed, we can easily derive upper and lower bounds by solving the LP relaxation (no need for local search). The core of the approach is an observation that, for a maximization task, if the upper bound for a subproblem l_1 is smaller than the lower bound for any other subproblem l_2, then l_1 and the branch rooted at l_1 can be safely discarded from the tree, such that the computational complexity can be reduced. This procedure is called *pruning*.

The algorithm terminates when the upper bound reaches $(1+\epsilon)$ of the lower bound. Let the optimal object value be

TABLE I
BRANCH-AND-BOUND ALGORITHM

	Initialization:
1	Obtain LP relaxation OPT-VBR(l) as Prob 1;
2	Set optimal solution $sol = \phi$, Problem list $\mathcal{S} = \{\text{Prob 1}\}$, $UB = \infty$, and $LB = 0$;
3	Solve Prob 1 for solution $\{\vec{P}', \vec{u}', \vec{\gamma}', \vec{v}'\}$ and upper bound UB_1;
4	Use $\vec{P}'$, (7), and (8) to get lower bound LB_1;
5	Set $UB = UB_1$ and $LB = LB_1$;
	Iteration & pruning:
6	Select Prob l with the largest UB_l in $\mathcal{S}$ and set $UB = UB_l$;
7	IF ($LB_l > LB$) {
8	Set $sol = \vec{P}'_l$ and $LB = LB_l$;
9	IF ($UB \leq (1+\epsilon)LB$) stop with solution sol;
10	ELSE remove all probs k in $\mathcal{S}$ with $UB_k \leq (1+\epsilon)LB$; }
	Partition:
11	For Prob l, find the maximum relaxation error among all RLT variables, e.g., $\max_{m,k}\{\lvert\gamma_m P_k - v_{mk}\rvert\}$;
12	Evaluate the following condition: $(\gamma_m^{max} - \gamma_m^{min}) \cdot \min\{\gamma'_m - \gamma_m^{min}, \gamma_m^{max} - \gamma'_m\} \geq (P_m^{max} - P_m^{min}) \cdot \min\{P'_m - P_m^{min}, P_m^{max} - P'_m\}$;
13	IF (true) partition $[\gamma_m^{min}, \gamma_m^{max}]$ into $[\gamma_m^{min}, \gamma'_m]$ and $[\gamma'_m, \gamma_m^{max}]$;
14	ELSE partition $[P_m^{min}, P_m^{max}]$ into $[P_m^{min}, P'_m]$ and $[P'_m, P_m^{max}]$;
	Bounding:
15	Solve the partitioned probs l_1 and l_2 to get solutions sol_{l_1}, sol_{l_2} and bounds UB_{l_1}, UB_{l_2}, LB_{l_1}, LB_{l_2};
16	Remove Prob l from $\mathcal{S}$;
17	IF ($(1+\epsilon)LB < UB_{l_1}$) add Prob l_1 into $\mathcal{S}$;
18	IF ($(1+\epsilon)LB < UB_{l_2}$) add Prob l_2 into $\mathcal{S}$;
19	IF ($\mathcal{S} = \phi$) stop;
20	ELSE go to Step 6;

$O \leq UB$, we have $LB \geq \frac{1}{1+\epsilon}UB \geq \frac{1}{1+\epsilon}O = (1 - \epsilon + \epsilon^2 - \epsilon^3 + \cdots)O \approx (1-\epsilon)O$, for $0 \leq \epsilon \ll 1$. The pseudo code for the branch-and-bound algorithm is given in Table I.

C. Enhancement

We introduce a heuristic to accelerate the convergence of the branch-and-bound algorithm. At the beginning of time slot t, if the playout buffer occupancy is above a certain threshold, say, 80%, and $X_m(t-1) \geq D_m(t)$ at user un_m, we set $P_m(t) = 0$ and remove the link from the optimization process.

Generally the playout buffer size should at least be greater than the largest frame size. Given the large variations in VBR frame sizes, there could be multiple frames stored when the buffer is close to full. When the above conditions are satisfied, there is little chance of buffer underflow at the end of time slot t even if we do not transmit anything to user un_m. On the other hand, if we schedule a non-zero power $P_m(t)$ for this link, only a small amount of bits can be transmitted due to the buffer overflow constraint, but at the cost of reduced SINRs at all other links. Excluding such links from transmission not only greatly speeds up the convergence of the branch-and-bound algorithm, but also increases the SINR and capacity of other active links.

IV. DISTRIBUTED ALGORITHM

Although the RLT-based branch-and-bound algorithm can provide a $(1-\epsilon)$-optimal solution, it requires a centralized implementation. A centralized controller is needed to collect network, link and video related information, and to update transmit power for each downlink. In this section, we develop a distributed algorithm for Problem OPT-VBR that can be implemented in each BS and operate with local information.

We assume each BS obtains video cumulative consumption curves and playout buffer sizes for its users during the video session initiation phase. At the beginning of time slot t, each BS m computes for user un_m the minimum rate as $[D_m(t) - X_m(t-1)]/\tau$, i.e., the data rate that empties the playout buffer at the end of time slot t but without underflow, and the maximum rate as $[B_m(t) - X_m(t-1)]/\tau$, i.e., the data rate that makes the playout buffer full at the end of time slot t but without overflow. BS m then translates the minimum and maximum rates to minimum and maximum SINRs, i.e., $\gamma_m^{min}(t)$ and $\gamma_m^{max}(t)$ as given in (6). In the following, we again drop the time slot index (t) to simplify notation.

To maximize objective function (7), BS m sets a target SINR as $\gamma_m^{tar} = \gamma_m^{max}$, and tries to achieve the target SINR by adjusting its transmit power. The problem then becomes a *Distributed Constrained Power Control* (DCPC) problem [10]. BS m first randomly sets its initial transmit power as $0 < P_m^0 \leq \bar{P}$. Let γ_m^i be the i-th SINR measurement at user un_m, which is fed back to BS m. BS m then uses the following DCPC algorithm to update its power after receiving the i-th SINR feedback:

$$P_m^i = \min\left\{\bar{P}, \frac{\gamma_m^{tar}}{\gamma_m^i} P_m^{i-1}\right\},\ i = 1, 2, \cdots. \tag{42}$$

If the γ_m^{tar}'s are feasible (see Section II-C), the power vector series $\{\vec{P}^0, \vec{P}^1, \cdots, \vec{P}^i, \cdots\}$ is proved to converge to a unique positive power vector satisfying the following equation [10]

$$\vec{P} = \min\left\{\vec{\bar{P}}, \mathbf{\Gamma}^{tar}(\mathbf{A}\vec{P} + \vec{\nu})\right\}, \tag{43}$$

where $\mathbf{\Gamma}^{tar} = \text{diag}\{\vec{\gamma}^{tar}\} = \text{diag}\{\gamma_1^{tar}, \gamma_2^{tar}, \cdots, \gamma_M^{tar}\}$. Furthermore, the converged power vector $\vec{P}^*(t)$ also achieves the target SINR $\gamma_m^{tar}(t)$ for each BS m. The convergence result is summarized as the following fact from [10].

Fact 2: With the DCPC algorithm (42), the transmit power vector converges to a unique positive power vector $\vec{P}^*$ satisfying (43). After convergence, either $\vec{P}^*$ achieves $\vec{\gamma}^{tar}$ or at least one of the components in $\vec{P}^*$ is equal to $\bar{P}$.

The pseudo code for the distributed DCPC algorithm is given in Table II, where α is a fraction in (0,1) and β is a positive integer. If BS m's transmit power remains at the maximum power $\bar{P}$ for β iterations, while the target SINR γ_m^{tar} is still not achieved, we reset the target SINR as $\gamma_m^{tar} = \gamma_m^{min} + \alpha \cdot (\gamma_m^{tar} - \gamma_m^{min})$ and restart the iterative update process. We choose $\alpha = 0.618$, the reciprocal of the *golden ratio*, and β from 2 to 5 in our simulations.

In practice, the path gains vary over time due to channel fading. It is possible that during some time slot, the transmission is not feasible even for the minimum required rate. It is nontrivial to test the feasibility of the target SINR vector $\vec{\gamma}^{tar}$ in a distributed manner with only local information. In fact, if the target SINR vector is infeasible, the problem of finding the largest set of links that can be supported at the given SINRs is proved to be NP-Complete [17]. Therefore, we adopt the following heuristic strategies to handle the case

TABLE II
DCPC ALGORITHM

	Initialization:
1	BS m obtains b_m, D_m, and B_m for user un_m;
2	BS m computes SINR bounds γ_m^{max} and γ_m^{min};
3	BS m sets $\gamma_m^{tar} = \gamma_m^{max}$ and $P_m(0) \in (0, \bar{P}]$;
	Iteration:
4	BS m receives SINR feedback γ_m^i and updates its power as: $P_m^i = \min\left\{\bar{P}, \left(\gamma_m^{tar}/\gamma_m^i\right) P_m^{i-1}\right\}$;
5	If (($P_m^i = \bar{P}$ for β iterations) & ($\gamma_m^i \neq \gamma_m^{tar}$)) reset the target SINR as: $\gamma_m^{tar} = \gamma_m^{min} + \alpha \cdot (\gamma_m^{tar} - \gamma_m^{min})$;
6	$i = i + 1$ and go to Step 4;

when the target SINR vector cannot be achieved by a feasible power assignment due to deep fading channels.

i) In the first time slot, if the DCPC algorithm does not converge in a certain number of steps, suspend the transmission of the video with the largest frame size for sometime and retry the algorithm.
ii) Adopt the acceleration enhancement as in the centralized algorithm, which is described in Section III-C.
iii) If the DCPC algorithm does not converge for the reduced γ_m^{tar} (see Line 5 in Table II), further reduce the target SINR as $\gamma_m^{tar} = \gamma_m^{min} + \alpha \cdot (\gamma_m^{tar} - \gamma_m^{min})$. If still no convergence when $\gamma_m^{tar} = (1+\epsilon) \cdot \gamma_m^{min}$, for $0 < \epsilon \ll 1$, all the links whose buffer will not be empty in the next time slot will pause their transmissions. Since the algorithm always tries to transmit as more data as possible (i.e., by setting a high target SINR whenever possible), it is highly likely that such links won't have buffer underflow in the following time slots.
iv) If all the above steps fail, the BS suspends its transmission and the user freezes the playout precess until the next time slot.

V. SIMULATION RESULTS

To evaluate the performance of the proposed algorithms, we simulate streaming VBR videos in a 7-cell wireless network. We assume the channels within a cell are orthogonal and inter-cell interference is the major limiting factor. The channel bandwidth is $B_w = 1$ MHz. The path gain averages are set to $\bar{G}_k^m = d_{km}^{-4}$, where d_{km} is the physical distance from BS k to user un_m. We assume Rayleigh fading channels in all the simulations, where the normalized path gain is exponentially distributed as $f(G_k^m) = \exp\{-G_k^m/\bar{G}_k^m\}$ for $G_k^m \geq 0$. The distance from a user to its corresponding BS is uniformly distributed from 100 m to 1000 m and the inter-cell BS distance is from 1600 m to 2000 m. The temperature is $T_0 = 290$ Kelvin and the equivalent noise bandwidth is also 1 MHz. The peak power constraint is $\bar{P} = 1$ Watt.

In each cell, the channel is dedicated to one mobile user for VBR video streaming. We assume BS's 1, 4 and 7 are streaming movie *Star Wars*, BS's 2 and 5 are streaming *NBC News*, and the remaining links 3 and 6 are transmitting *Tokyo Olympics*. We use the VBR traces for these videos from the Video Trace Library hosted at Arizona State University [11] in all the simulations. The playout buffer size is set to be 1.5 times of the largest frame size in the requested VBR video.

A. Centralized Algorithm

We implement the branch-and-bound centralized algorithm using MATLAB. We choose $\epsilon = 10\%$ for the simulations. From the VBR video traces, we derive the cumulative consumption and overflow curves. The centralized algorithm computes the optimized power assignment for the BS's at beginning of each time slot. In Fig. 4(a), we plot the cumulative consumption, overflow and transmission curves for *Star Wars* transmitted on link 1. The top subfigure is for 10,000 frames. We also plot the curves from frame 1,960 to frame 1,980 in the bottom subfigure, while frame 1,969 has the largest size among the 10,000 frames. We observe that the cumulative transmission curve $X_1(t)$ is very close to the cumulative overflow curve $B_1(t)$, indicating that the centralized algorithm always aims to maximize the transmission rate as allowed by the buffer and power constraints, and the playout buffer is fully utilized for most of the time. There is no playout buffer overflow or underflow for the entire range of the movies.

In Fig. 5, we plot the upper and lower bounds for objective function (7) for time slot 1. This is the hardest time slot with respect to power control, since all the sessions are transmitting I-frames and all the playout buffers are empty in this time slot in our simulations. We observe the optimality gap between UB and LB is continuously decreased until the $\epsilon = 0.1$ threshold is reached. In other time slots where the frame sizes are not consistently large and the playout buffers are close to full, it usually takes only a few (e.g., 5 or 6) iterations to reach the optimality gap threshold.

We also evaluate the accelerated scheme under the same video and network conditions. The curves for link 1 are plotted in Fig. 4(b). It can be seen that during time slots 1,963, 1,967, and 1,971, there is no transmission on link 1 since the playout buffer is over 80% full. Pausing transmission in these time slots makes it easier for other links to transmit large frames and speeds up the convergence of the algorithm, while causing no buffer underflow at link 1. Since usually large frames rarely occur in the same time slot (except for time slot 1), this is analogous to statistical multiplexing of VBR videos. We find in the simulation, a link can pause in over 60% of the time slots with the acceleration heuristic, resulting in significant reduction in computation time.

B. Distributed Algorithm

We next examine the performance of DCPC. The network and video setups are the same as those in the centralized algorithm simulations. The cumulative overflow, transmission, and consumption curves obtained by DCPC are plotted in Fig. 4(c) for *Star Wars* transmitted on link 1. We observe very similar performance as in the case of the centralized algorithm shown in Fig. 4(a). The cumulative transmission curve is again very close to $B_m(t)$, and there is neither buffer overflow nor underflow during the transmission of 10,000 frames.

To compare the distributed and centralized algorithms, we compute the sum of the bit rates of all the links in each time slot. The acceleration scheme is not used for both algorithms in this simulation. The rate sums are plotted in Fig. 6(a)

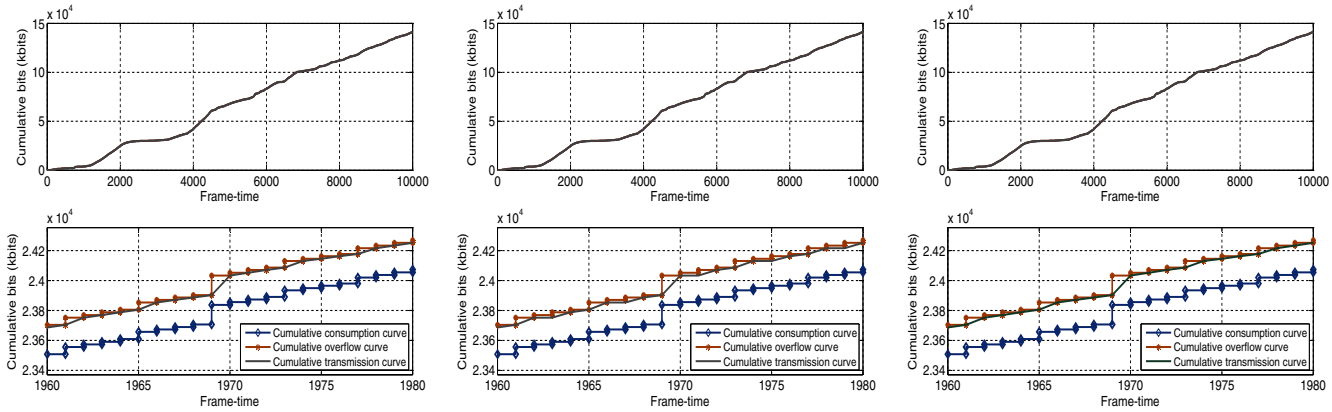

(a) Centralized algorithm (b) Accelerated centralized algorithm (c) DCPC

Fig. 4. The cumulative overflow, transmission, and consumption curves when transmitting *Star Wars* at link 1 in the seven-cell network.

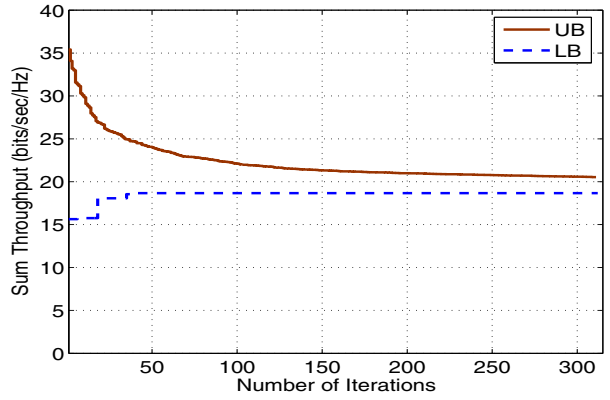

Fig. 5. Convergence of the branch-and-bound algorithm in time slot 1 when all the I-frames are transmitted and all the buffers are empty (i.e., the worst case scenario).

from time slot 6,800 to 6,840. We observe that the sum rates achieved by the centralized algorithm and that by the distributed algorithm are identical for most part of this interval. Examining the rate sums for the entire 10,000 time slots, we find that the rate sum achieved by the DCPC algorithm is within 99% of the corresponding rate sum achieved by the centralized algorithm in over 97% of the time slots.

The convergence of the distributed DCPC algorithm is plotted in Figs. 6(b) and 6(c) for one of the time slots. The accelerated scheme is incorporated with DCPC, such that a link m may pause its transmission if its buffer is over 80% full and $X_m(t-1) > D_m(t)$. The evolution of the BS transmit powers are plotted in Fig. 6(b), where after 23 steps, all the transmit powers converges to a value between 0 and $\bar{P} = 1$ Watt. The converged power vector is $\vec{P}^*$ = [0.0023, 0.208, 0.185, 0.0013, 0.163, 7.1×10^{-04}, 0.188] Watt. The evolution of the bit rates are plotted in Fig. 6(c). It is interesting to see the data rates converge faster than the transmit powers in this case. All the data rates reach stable values after a few steps.

VI. Related Work

Most of the prior work on VBR video streaming consider wired networks, which can be classified according to their traffic models, i.e., *statistical* or *deterministic* models. With the former approach, stochastic models are developed to capture the burstiness in VBR traffic. In [2], [3], the authors observed the *long-range-dependence* in VBR video traffic and modeled the autocorrelation with self-similar processes. This class of work provides valuable insights on the nature of VBR video traffic. The stochastic models can be incorporated in QoS mechanisms for VBR videos, and for traffic synthesizing in simulations [18].

With the deterministic approach, the piecewise-constant-rate transmission and transport (PCRTT) method was used, aiming to optimize one or more objectives while preserving continuous video playout. In [4], Liew and Chan proposed bandwidth allocation schemes for dynamically sharing a CBR channel among multiple VBR video streams, either i) to minimize the total receiver buffer size, or ii) to avoid underflow and overflow for a given playout buffer size. In [5], Salehi *et al.* considered smoothing VBR video over a CBR link and developed an effective algorithm to achieve the greatest smoothness in rate. In [19], McManus and Ross introduced a dynamic programming framework to set PCRTT rates and intervals to optimize different objective functions. These techniques do not directly apply to our problem of VBR over multicell wireless networks, due to the fundamental difference between wireless and wired CBR links.

In two recent papers [20] and [7], the authors studied the more challenging problem of transmitting one VBR video over a given time-varying (i.e., VBR) wireless channel. In [20], it was shown that the separation between a delay jitter buffer and a decoder buffer is in general suboptimal, and several critical parameters are derived for the system. In [7], the authors studied the frequency of jitters under both network and video system constraint and provided a framework for quantifying the trade-offs among several system parameters. In this paper, we take advantage of power control in wireless networks to adjust the capacity of wireless links based on video frame size information, such that we can jointly optimize the transmission of *multiple* VBR video sessions over *multiple* VBR channels. Our approach does not depend on any channel or video traffic

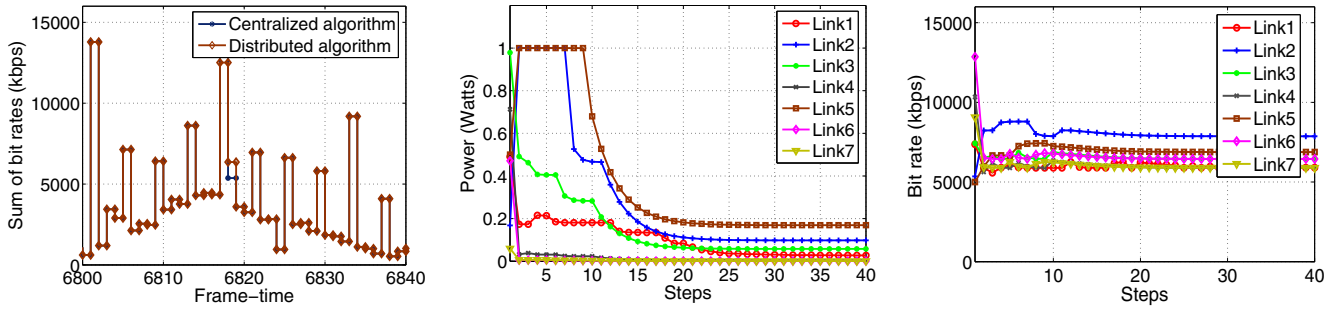

(a) Rate sums with the algorithms (b) Convergence of transmit powers with DCPC (c) Convergence of bit rates with DCPC

Fig. 6. Simulation results with a seven-link network.

models, and can be adopted for CBR video as well.

Power control is an important problem for interference-limited wireless networks. Most prior work focuses on maximizing network utility in the forms of SINR or bit rate [8]–[10]. In [10], Grandhi, Zander, and Yates presented centralized and distributed power control algorithms for achieving target SINRs in a cellular network. In [8], Chiang studied the problem of joint power control and congestion control, aming to maximize the throughput of TCP-Vegas over an ad hoc network. Gjendemsj *et al.* [9] presented centralized binary power control algorithms for maximizing the sum rate over multiple interfering links. Although laid out the theoretical foundation and developed effective algorithms, these techniques cannot be directly applied for VBR video over multicell wireless networks with buffer and delay constraints.

VII. Conclusion

We studied downlink power control for VBR video streaming in multicell wireless networks. The problem formulation considers downlink power control, inter-cell interference, VBR video characteristics, and playout buffer requirements. We developed a centralized algorithm that can provide (1-ϵ)-optimal solutions, and a fast distributed algorithm that only needs local information. The algorithms are evaluated with extensive simulations with VBR video traces and fading channels, and are demonstrated to be effective for streaming VBR videos over multicell wireless networks.

Acknowledgment

This work is supported in part by the US National Science Foundation (NSF) under Grants ECCS-0802113, NSF-CNS-0953513, and NSF-IIP-1032002, and through the Wireless Internet Center for Advanced Technology (WICAT) at Auburn University. Any opinions, findings, and conclusions or recommendations expressed in this material are those of the author(s) and do not necessarily reflect the views of the NSF.

References

[1] Cisco, "Cisco visual networking index: Global mobile data traffic forecast update, 2009-2014," Feb. 2010, [online] Available: http://www.cisco.com.

[2] M. W. Garrett and W. Willinger, "Analysis, modeling and generation of self-similar VBR video traffic," *ACM SIGCOMM Comput. Commun. Rev.*, vol. 24, no. 4, pp. 269–280, 1994.

[3] J. Beran, R. Sherman, M. Taqqu, and W. Willinger, "Long-range dependence in variable-bit-rate video traffic," *IEEE Trans. Commun.*, vol. 43, no. 2/3/4, pp. 1566–1579, Feb./Mar./Apr. 1995.

[4] S. Liew and H. Chan, "Lossless aggregation: a scheme for transmitting multiple stored VBR video streams over a shared communications channel without loss of image quality," *IEEE J. Sel. Areas Commun.*, vol. 15, no. 6, pp. 1181–1189, Aug. 1997.

[5] J. Salehi, Z.-L. Zhang, J. Kurose, and D. Towsley, "Supporting stored video: reducing rate variability and end-to-end resource requirements through optimal smoothing," *IEEE/ACM Trans. Networking.*, vol. 6, no. 4, pp. 397–410, Aug. 1998.

[6] S. Sen, D. Towsley, Z. Zhang, and J. K. Dey, "Optimal multicast smoothing of streaming video over the internet," *IEEE J. Sel. Areas Commun.*, vol. 20, no. 7, pp. 1345–1359, Sep. 2002.

[7] G. Liang and B. Liang, "Balancing interruption frequency and buffering penalties in VBR video streaming," in *Proc. IEEE INFOCOM'07*, Anchorage, AK, May 2007, pp. 1406–1414.

[8] M. Chiang, "Balancing transport and physical layers in wireless multihop networks: jointly optimal congestion control and power control," *IEEE J. Sel. Areas Commun.*, vol. 23, no. 1, pp. 104–116, Jan. 2005.

[9] A. Gjendemsj, D. Gesbert, G. Oien, and S. Kiani, "Binary power control for sum rate maximization over multiple interfering links," *IEEE Trans. Wireless Commun.*, vol. 7, no. 8, pp. 3164–3173, Aug. 2008.

[10] S. Grandhi, J. Zander, and R. Yates, "Constrained power control," *Int. J. Wireless Personal Commun.*, vol. 1, no. 4, pp. 257–270, Apr. 1995.

[11] M. Reisslein, "Video trace library," Arizona State University, [online] Available: http://trace.eas.asu.edu/.

[12] M. Chen and A. Zakhor, "Multiple TFRC connections based rate control for wireless networks," *IEEE Trans. Multimedia*, vol. 8, no. 5, pp. 1045–1062, Oct. 2006.

[13] J. Lee, R. Mazumdar, and N. Shroff, "Downlink power allocation for multi-class wireless systems," *IEEE/ACM Trans. Networking*, vol. 13, no. 4, pp. 854–867, Aug. 2005.

[14] N. Bambos, S. C. Chen, and G. J. Pottie, "Radio link admission algorithm for wireless networks with power control and active link quality protection," in *Proc. IEEE INFOCOM'95*, Boston, MA, Apr. 1995, pp. 97–104.

[15] H. D. Sherali and W. P. Adams, *A Reformulation-Linearization Technique for Solving Discrete and Continuous Nonconvex Problems*. London, UK: Kluwer Academic Publishers, 1999.

[16] S. Kompella, S. Mao, Y. Hou, and H. Sherali, "On path selection and rate allocation for video in wireless mesh networks," *IEEE/ACM Trans. Netw.*, vol. 17, no. 1, pp. 212–224, Feb. 2009.

[17] M. Andersin, Z. Rosberg, and J. Zander, "Gradual removals in cellular PCS with constrained power control and noise," in *Proc. IEEE PIMRC'95*, Toronto, Canada, Sept. 1995, pp. 56–60.

[18] D. P. Heyman and T. V. Lakshmanr, "What are the implications of long-range dependence for VBR-video traffic engineering?" *IEEE/ACM Trans. Networking*, vol. 4, no. 3, pp. 301–317, June 1996.

[19] J. M. Mcmanus and K. W. Ross, "A dynamic programming methodology for managing prerecorded vbr sources in packet-switched networks," in *in Proceedings SPIE, Performance and Control of Network Systems*, 1997, pp. 140–154.

[20] T. Stockhammer, H. Jenkac, and G. Kuhn, "Streaming video over variable-bit-rate wireless channels," *IEEE Trans. Multimedia*, vol. 6, no. 2, pp. 268–277, Apr. 2004.